

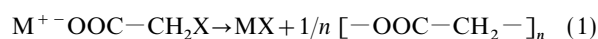
Polyglycolide with controlled porosity: an improved biomaterial

Matthias Epple* and Oliver Herzberg

Institute of Inorganic and Applied Chemistry, University of Hamburg, Martin-Luther-King-Platz 6, D-20146 Hamburg, Germany

A method to prepare polyglycolide, the simplest polyester, with defined microstructure by solid-state polymerization of halogenoacetates is presented. By choosing the appropriate halogenoacetate it is possible to obtain polyglycolide with variable porosity. The pore size distribution can be varied by choice of the precursor and an appropriate mechanical pretreatment (average pore diameters between 0.3 and 1.5 μm). Porous polyglycolide should degrade faster in the environment or in the body than compact polyglycolide. Alternatively, microcrystals of the eliminated salts can be obtained by extracting the polyglycolide. Thermodynamic data for halogenoacetates are given.

Polyglycolide [poly(oxy-1-oxoethylene)], the simplest polyester, can be prepared by elimination of metal halides from halogenoacetates at moderate temperatures [eqn. (1)].



We have reported earlier on mechanistic studies of this reaction by various solid-state chemical methods.¹⁻⁶ All results so far point to a pure solid-state reaction without intermediates or by-products.

Due to deposition of microcrystals of the eliminated salt in the polymeric matrix, a 'composite' of metal halide and polyglycolide is obtained. Simply washing out the salt with water leaves a highly porous polyglycolide. As polyglycolide, together with its higher homologues like polylactide, is under investigation as a biomaterial, e.g., for bone fixation screws,^{7,8} surgical sutures⁹ or controlled-rate drug release devices,¹⁰ control of its micromorphology and porosity would be of high interest. Its insolubility at ambient temperature in practically all solvents except for 1,1,1,3,3,3-hexafluoroisopropyl alcohol¹¹ makes it interesting as a highly inert material. It is non-toxic, readily degradable in the body or the environment and yet possesses a good mechanical strength.

Conventionally, polyglycolide is prepared from solution,¹¹ and thus has a compact structure, in contrast to the porous polyglycolide from the solid-state reaction. Here, we describe how porosity and pore size in polyglycolide can be varied by choice of the appropriate halogenoacetate and the appropriate pretreatment.

Polymerizability of halogenoacetates with different metal cations and halogen substituents

A number of halogenoacetates of the general formula MOOCCH_2X (M = monovalent metal; X = halogen) were prepared and studied in terms of their thermal polymerizability by differential scanning calorimetry (DSC) and simultaneous thermogravimetry-differential thermal analysis-mass spectrometry (TG-DTA-MS). Together with the results reported in an earlier publication,³ we now have an almost complete picture of the thermochemical reactivity of salts with $\text{M} = \text{Li}, \text{Na}, \text{K}, \text{Rb}, \text{Cs}, \text{Ag}$ and $\text{X} = \text{Cl}, \text{Br}, \text{I}$ and results are shown in Table 1. In 13 out of 17 cases, quantitative polymerization occurs, the exceptions being for lithium salts and sodium iodoacetate.

Lithium halogenoacetates do not polymerize: they either melt undecomposed or decompose without melting. As the

Table 1 Polymerizability of halogenoacetates

	Cl	Br	I
Li	—	—	—
Na	+	+	—
K	+	+	+
Rb	+	+	+
Ag	+	+	unstable
Cs	+	+	+
NH ₄	(+) ^a	not studied	not studied

^aAmmonium chloroacetate oligomerizes in the melt, i.e. not in a solid-state reaction.

driving force for the reaction is probably the high lattice energy of the eliminated salt MX , and as lithium halides have high lattice energies, we assume that the reason for this inertness lies in the crystal structure of the lithium halogenoacetates. Possibly the crystal structure of the lithium salts does not support the desired elimination reaction due to unfavourable packing. Unfortunately, except for silver chloroacetate⁵ and sodium chloroacetate,¹² none of the crystal structures is known, due to the difficulty in preparation of single crystals of halogenoacetates. We assume that the strong polarizing effect of the small lithium cation leads to a different packing in the crystal. In the case of sodium iodoacetate the strongly exothermic reaction leads to self-heating and combustion.

Thermodynamical data are collected in Table 2 and upon close inspection some remarkable trends are revealed. First, the stability of the compounds towards polymerization

Table 2 Onset temperatures ($^{\circ}\text{C}$) and reaction enthalpies (kJ mol^{-1}) for the polymerization reaction (by DSC; 5 K min^{-1}) leading to solid polyglycolide^a

	Cl	Br	I
Li	211/+11.2 ^b	210/+16.6 ^b	220/— ^c
Na	198/−25.2	186/−23.4	204/−72.0 ^d
K	157/−40.3	171/−36.9	192/−23.5
Rb	120/−42.5	99/−25.4 ^e	114/−24.4
Ag	134/−64.2	78/−63.9	unstable
Cs	<25/— ^f	35/−26.9 ^g	86/−35.7

^aValues for ammonium chloroacetate are 107°C and $-21.8 \text{ kJ mol}^{-1}$.

^bEndothermic melting followed by exothermic decomposition. ^cNo melting; exothermic decomposition. ^dProbably polymerization, leading to self-heating and combustion. ^eTwo peaks at 99 and 142°C (see Experimental section). ^fPolymerization occurs below room temperature. ^gSample had partially reacted before the experiment. The exothermic polymerization is followed by an endothermic peak (see Experimental section).

* Email: epple@xray.chemie.uni-hamburg.de

increases when going from the lower left corner (Cs/Cl) to the upper right corner (Li/I), as demonstrated by the reaction temperature. Similarly, the (negative) reaction enthalpy shows a decreasing trend when going from the lower left corner (Cs/Cl) to the upper right corner (Li/I). Interestingly, the silver compounds may be inserted between the alkali metals rubidium and caesium according to the position of silver in the Periodic Table.

The reason for these trends is not known. It may result from either crystallography (packing) or other thermodynamic factors. Without having exact values for enthalpies of formation or knowledge of the crystal structures, any explanation would be highly speculative. No thermodynamic data of halogenoacetates are available in the literature.

We carried out the polymerization of sodium and potassium chloroacetate using a high-pressure DSC instrument under 50 bar of nitrogen. Neither the enthalpy of reaction nor reaction temperature showed a notable difference from experiments at ambient pressure. This suggests that the rate determining step of the reaction does not involve a large change in volume.

Control of porosity of polyglycolide

Even though we cannot, at this point, readily explain why only some halogenoacetates polymerize, polyglycolide can be obtained conveniently from 11 different precursors (all substances in Table 2 except for the lithium salts, sodium iodoacetate, caesium chloroacetate and bromoacetate). The formed metal halide is easily extracted by washing with water (in the case of the silver salts, complexing agents must be added for dissolution). The overall porosity of the remaining polyglycolide can be controlled by choice of the appropriate precursor. We present below a method to predict the resulting porosity.

We did not determine the density of the halogenoacetates, however, the porosity can be estimated under the assumption that the partial volume occupied by the metal M and the halogen X is constant during the reaction. If so, the partial volume of the salt MX occupied in the reaction product is given by eqn. (2),

$$\frac{V_m(\text{MX})}{V_m(\text{MXAc})} = \frac{w(\text{MX})}{w(\text{MX}) + [1 - w(\text{MX})]\rho(\text{MX})/\rho(\text{PG})} \quad (2)$$

where $V_m(\text{MX})$ is the molar volume occupied by the metal salt MX in the reaction product, $V_m(\text{MXAc})$ is the molar volume of the halogenoacetate which is equal to the volume of the reaction product, $w(\text{MX})$ is the mass fraction of MX in the halogenoacetate, *i.e.* $M(\text{MX})/M(\text{MXAc})$, $\rho(\text{MX})$ is the density of MX (tabulated) and $\rho(\text{PG})$ is the density of the formed polyglycolide.

This derivation follows immediately from the assumption that

$$V_m(\text{MXAc}) = V_m(\text{MX}) + V_m(\text{PG}) \quad (3)$$

The porosity of the remaining polyglycolide after washing out the salt is equal to the ratio $V_m(\text{MX})/V_m(\text{MXAc})$. The density of polyglycolide was determined previously to be 1.707 g cm^{-3} (crystalline) or 1.50 g cm^{-3} (amorphous).¹¹ From the melting peak by DSC and the observation of diffraction peaks in the X-ray powder diffraction pattern we estimated the crystallinity of the formed polyglycolide to be *ca.* 50% (see below). Taking this into account, we estimated the density of polyglycolide to be 1.6 g cm^{-3} . For silver chloroacetate we obtained a density of 3.25 g cm^{-3} in good agreement with the X-ray density of 3.219 g cm^{-3} .⁵

For the 11 halogenoacetates mentioned above the porosity is lowest for silver chloroacetate (41.6%). It increases to 42.6% for sodium chloroacetate and 54.5% for potassium bromoacetate, and to a maximum of 62.3% for rubidium iodoacetate. Interestingly, an increasing mass fraction of MX in

the halogenoacetate is partly compensated by a higher density of the formed MX.

Control of pore size distribution in polyglycolide

The next point we address is the pore size distribution in the polyglycolide formed, whether it depends on the precursor, or it can be controlled by varying the synthesis conditions (*e.g.*, reaction temperature, reaction extent, pressure, mechanical pretreatment). We studied this by preparing different samples of polyglycolide by solid-state reaction and investigating their morphology by scanning electron microscopy (SEM) at magnifications of 10^2 – 10^4 . Representative parts of the surface were examined under different magnifications and pores were counted and measured. The major results for polyglycolide obtained from previously ground halogenoacetate are given in Table 3.

The obtained values show a considerable scatter; the only trends that may cautiously be stated is that the number of pores and the average pore diameter are inversely proportional to each other and that heavier metal halides promote the formation of fewer but larger pores. The presence of large pores (diameter $>1 \mu\text{m}$) is probably of interest for use in membranes; this parameter can be varied by choice of the precursor between 0 and 8–9 pores per $100 \mu\text{m}^2$. Fig. 1 shows three representative SEM micrographs.

The observed scatter is not unexpected since the pore size distribution is likely to depend not only on the precursor but also on the reaction temperature which differs for each precursor. We have varied the reaction temperature and time for sodium bromoacetate and found the following results for three completely reacted samples: 100/60/45 min at 170/180/190 °C: 460/90/18 pores per $100 \mu\text{m}^2$, with average pore diameter 0.3/0.5/0.9 μm . The sodium bromide crystallites seem to coalesce at higher temperature. This may arise from the need to minimize the surface energy. The mobility of the M^+ and X^- ions must be high at the reaction temperature as demonstrated by the formation of macroscopic MX crystals during the reaction, a process which requires extensive diffusion. This result demonstrates that the pore size distribution is variable even when using the same precursor.

The strongest influence on the polyglycolide morphology was mechanical pretreatment of the halogenoacetate. We found that ground sodium chloroacetate produced many small pores whereas polycrystalline sodium chloroacetate as obtained from solution without further treatment had fewer pores, but with larger diameters: for ground/polycrystalline material we obtained the following results after 100/60 min at 185/180 °C: 258/75 pores per $100 \mu\text{m}^2$ with an average pore diameter of 0.3/0.8 μm and 0.0/5.3 pores larger than $1 \mu\text{m}$ per $100 \mu\text{m}^2$.

This observation can be explained by the well known fact that solids tend to form the first nuclei at defects in the regular crystal structure where the local energy is increased.^{13,14} By grinding the sodium chloroacetate obtained from solution the number of lattice defects and distortions increases, and thereby the number of potential nuclei. Upon heating, the reaction

Table 3 Pore size distribution of porous polyglycolide from different halogenoacetates (by SEM, 100% reaction extent; halogenoacetates ground prior to the reaction). Entries: total number of pores per $100 \mu\text{m}^2$ /number of pores with diameter $>1 \mu\text{m}$ per $100 \mu\text{m}^2$ /average maximum pore diameter from number average/reaction temperature (°C)

	Cl	Br	I
Na	260/0.0/0.3/185	460/2.3/0.3/170	—
K	280/0.2/0.3/190	855/0.9/0.3/195	14/5.8/1.5/175
Rb	30/5.9/1.1/120	260/6.6/0.4/90	90/8.4/0.8/130
Ag	240/0.3/0.4/130	17/2.4/0.9/100	—
Cs	—	—	65/9.6/0.9/100

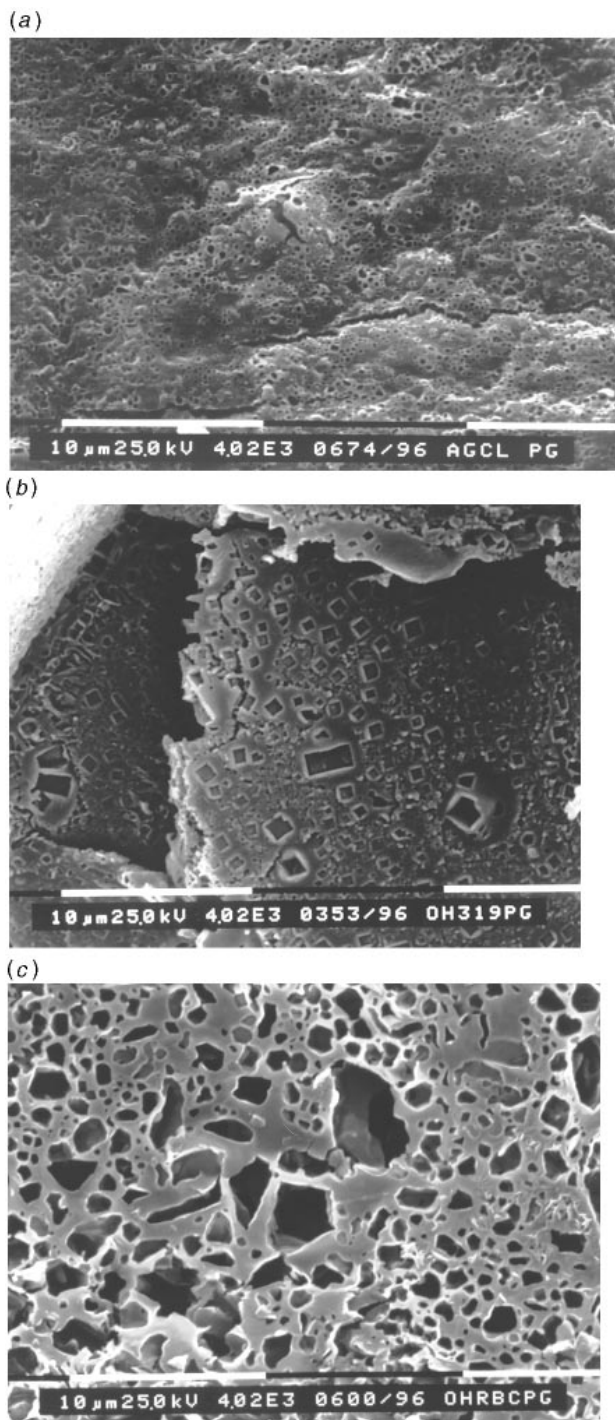


Fig. 1 Scanning electron micrographs of porous polyglycolide obtained from silver chloroacetate at 130 °C (a), from sodium bromoacetate at 180 °C (b) and from rubidium chloroacetate at 120 °C (c). All samples were ground prior to the reaction (magnification 4020×).

commences at more sites as compared to more highly crystalline material. If we assume that the number of the sodium chloride crystals formed is proportional to the number of nuclei, it follows that many nuclei must lead to many small NaCl crystals and that fewer nuclei must lead to fewer but larger NaCl crystals.

This observation shows that it is possible to adjust the pore size in polyglycolide by merely grinding the halogenoacetate before reaction. This possibility seems more attractive than varying the precursor, given that sodium chloroacetate is an inexpensive chemical (*ca.* 40 \$ kg⁻¹) that can be prepared easily.

We do not know exactly how the pores are connected, but the observation that the formed metal salt MX can be extracted quantitatively by washing with water points to the fact that all pores are interconnected, *i.e.* no isolated MX crystals exist. This is important for a potential use of porous polyglycolide as a membrane.

The degree of crystallinity of the formed polyglycolide can be estimated from the ratio of the measured melting enthalpy to the enthalpy of a fully crystalline sample. The melting enthalpy for 100% crystalline polyglycolide has been calculated to 11.96 kJ mol⁻¹.¹⁵ Using this value, we obtained crystallinities of between 30 and 60% for the different samples. No correlation between crystallinity and composition or reactivity of halogenoacetate could be observed. The high crystallinity is confirmed by X-ray powder diffraction (XRD) where polyglycolide gave strong peaks at 2θ 21.1, 22.1, 25.4, 28.3, 30.8, 35.8, 39.3, 41.0, 42.3 and 47.9° (Cu-Kα radiation; λ = 1.541 78 Å). No differences between the polyglycolide samples were found according to XRD.

Salt microcrystals

Interestingly, if the polyglycolide is extracted from a reacted halogenoacetate with hot 1,1,1,3,3,3-hexafluoroisopropyl alcohol, the salt crystals that once formed the pores remain and can be filtered off. Fig. 2(a) shows an SEM micrograph of NaBr microcrystals formed from reacted sodium bromoacetate. The crystals are of an almost uniform size and are of cubic

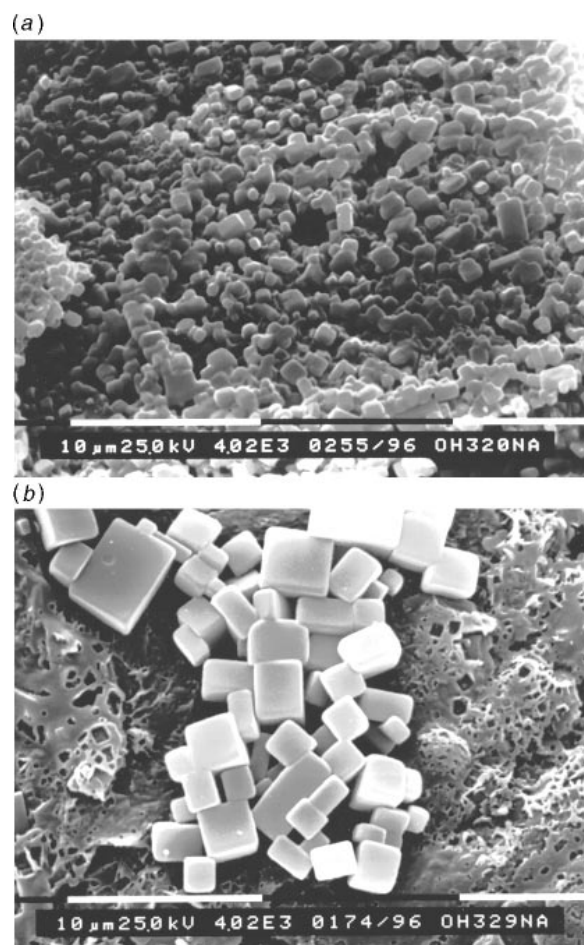


Fig. 2 Salt microcrystals obtained after converting a halogenoacetate to polyglycolide and salt and washing out the polymer with 1,1,1,3,3,3-hexafluoroisopropyl alcohol. (a) NaBr microcrystals from sodium bromoacetate; (b) NaCl on polyglycolide from sodium chloroacetate (partial removal of polyglycolide) (magnification 4020×)

shape, however, the smaller crystals are likely to have gone through the filter.

This is corroborated by Fig. 2(b) where NaCl crystals on a polyglycolide surface are displayed. This sample arose from incomplete removal of polyglycolide. The NaCl crystals are generally larger than the polyglycolide pores, a fact that we ascribe to loss of the smaller NaCl crystals during filtering and possibly Ostwald ripening, *i.e.* growth of larger crystals on the expense of smaller ones, during extraction with hot 1,1,1,3,3,3-hexafluoroisopropyl alcohol. Similar morphologies were obtained for salts from other halogenoacetates.

The crystals show round edges, indicative of the low-temperature synthesis that led to their production, *i.e.* at too low a temperature for surface defects to heal. As well as preparing porous polyglycolide, one can also thus prepare fairly homogeneous microcrystals of alkali-metal and silver halogenides.

Preparation of larger polyglycolide particles

All results reported above were obtained for materials with particle sizes of *ca.* 1–50 μm . For any practical application, it is indispensable to have larger samples with dimensions of milli- or centimetres. We thus investigated whether this could be accomplished.

All the elimination reactions are highly exothermic in nature (Table 2) and this makes it almost impossible to react larger (compact) samples of a halogenoacetate. Even with the utmost care in heating, autocatalytic self-heating occurs that leads to melting of the polyglycolide and often also to combustion. This may happen also with powders if the heating is too rapid. However, powders can usually be reacted without problems.

There are two possible ways to obtain larger polyglycolide particles, both *via* the reacted powders. The first is to prepare polyglycolide + metal salt from a powdered sample, to melt it carefully and let it solidify in a desired mould. The metal salt can then be removed with water without destroying the macroscopic geometry of the polyglycolide. Because polyglycolide tends to decompose when molten, melting must be done carefully.

The second method is based on pressing reacted powdered polyglycolide + metal salt into a pellet. We found that a common IR press works very well for this purpose (10 tonnes pressure; 14 mm diameter). The sodium chloride can be removed quantitatively by washing three times with warm water, followed by ethanol and drying *in vacuo*. This demonstrates that the interconnecting pore system is not damaged by the pressing. The effective density of such a polyglycolide pellet is 0.68 g cm^{-3} . This procedure is shown schematically in Fig. 3.

If the sodium chloride is removed from the polyglycolide powder before the pressing, the pore structure does not withstand the pressure, as shown by the effective density of 1.34 g cm^{-3} for such a pellet. A similar density was obtained for a pellet prepared from molten polyglycolide powder. The density difference between porous and dense material is in good agreement with the porosity estimates presented above. Scanning electron micrographs of surfaces and fractured sections of such a porous pellet confirm its hollow structure.

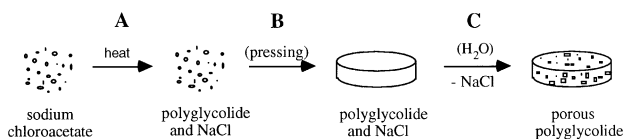


Fig. 3 Schematic procedure to a porous polyglycolide pellet from sodium chloroacetate: a powder of sodium chloroacetate is reacted thermally (A) and pressed to a pellet (B). Washing out the NaCl with water (C) leaves a porous pellet.

A pellet of porous polyglycolide is surprisingly not brittle and appears to be as mechanically stable as a compact pellet. To quantify the mechanical properties, we carried out thermo-mechanical analysis (TMA) with an oscillating load. Two samples were subjected to this experiment: a pellet of porous polyglycolide prepared as in Fig. 3 and a pellet of compacted polyglycolide obtained by compacting a porous polyglycolide powder, *i.e.* crushing the pore structure. The samples were heated up from 25 to 210 °C at 2 K min^{-1} and subjected to a load that oscillated between 0.05 and 0.15 N (period 12 s; quartz sensor area 7 mm^2). Both samples behave almost equally: the elasticity remains constant between 25 and 150 °C and no permanent deformation occurs. The elasticity (Young's modulus) is of the order of $(3\text{--}5) \times 10^6 \text{ Pa}$ for both samples. Above 150 °C, both samples begin to shrink slowly at first, then rapidly above 200 °C due to the onset of melting. The total shrinkage between 150 and 200 °C is *ca.* 5%.

These results show that the porous structure is completely stable up to 150 °C and that it is almost stiff, *i.e.* is not deformed or relaxed under changing pressure; otherwise, the elasticity modulus of the porous sample would have been much smaller than that of the compact sample, therefore resulting in a higher deformation of the porous pellet.

Polyglycolide from a solvate

It is known that halogenoacetates tend to crystallize as solvates that include free acid into the crystal lattice.^{16,17} We have reported earlier on *in situ* studies on rubidium bromoacetate–bromoacetic acid (1/1) that gave hints on the formation of polyglycolide in such compounds.¹⁸ Rubidium bromoacetate solvate reacted in two steps: first the bromoacetic acid was released, then the remaining rubidium bromoacetate polymerized to polyglycolide. In this case, we were unable to isolate the polymer. In the light of these studies we prepared potassium bromoacetate–bromoacetic acid (2/1). This compound releases bromoacetic acid at *ca.* 125 °C followed by exothermic polymerization and we were able to isolate polyglycolide + KBr after the reaction. Washing out KBr with water left a porous polyglycolide as in the case of the pure halogenoacetates.

An SEM micrograph of such a sample is shown in Fig. 4. The sample has a very uneven surface with many large pores visible. This may be due to simultaneous release of bromoacetic acid and solid-state polymerization, leading to strong turbulence and disorder during the synthesis. We found 40 pores per $100 \mu\text{m}^2$ with an average pore diameter of 0.9 μm and 7.8 pores larger than 1 μm per $100 \mu\text{m}^2$.

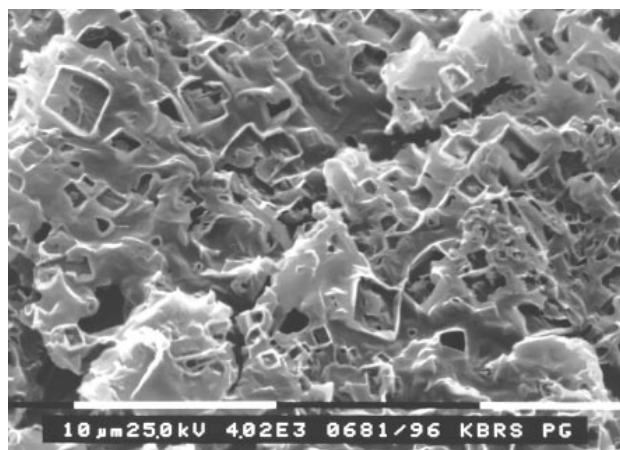


Fig. 4 Porous polyglycolide obtained from potassium bromoacetate–bromoacetic acid (2/1) by annealing at 120 °C and washing with water. The surface is rugged due to simultaneous desolvation and polymerization (magnification 4020 ×).

Conclusions

Most halogenoacetates undergo a solid-state polymerization reaction under elimination of metal halogenides when heated to moderate temperatures. As reaction product, an intimate mixture of bulk polyglycolide and small metal salt crystals is obtained. The metal salt can be removed by washing with water, leaving a highly porous polyglycolide. We have shown that it is possible to control porosity as well as pore size distribution by choice of the appropriate halogenoacetate precursor, by varying the reaction temperature and by mechanical treatment of the precursor before the reaction. Manufacture of larger polyglycolide samples is possible by pressing reacted powder and washing out the water. Such pellets possess a high mechanical stability as well as a good chemical resistance, due to the insolubility of polyglycolide in almost all solvents. Possible applications for tailor-made porous polyglycolide could be in medicine (e.g. bone substituent), in membrane technology or in pharmacology (controlled-release drugs).

Experimental

Instruments and methods

For differential scanning calorimetry, a calibrated^{19–21} Mettler DSC 27 HP high-pressure heat-flux calorimeter was used (operated at ambient pressure unless otherwise stated). We used aluminium capsules whose lid was pierced with a needle as sample holders (typical sample mass 5–10 mg; heating rate 5 K min⁻¹). Reported temperatures correspond to peak onsets.¹⁹

Simultaneous thermogravimetry, differential thermal analysis and mass spectrometry of evolved gases was carried out on a Netzsch STA 409/Balzers QMS 421 system. Samples (50–150 mg) were placed in open alumina crucibles and heated under dynamic air atmosphere (50 ml min⁻¹; 5 K min⁻¹). Mass fragments at *m/z* 18 (H₂O) and *m/z* 44 (CO₂) were detected in all experiments during combustion and are not explicitly listed below.

For X-ray powder diffractometry we used a Philips PW1050/25 diffractometer with nickel-filtered Cu-K α radiation ($\lambda = 1.54178$ Å) equipped with a proportional counter.

High-resolution solid-state CP MAS NMR was carried out on a Bruker MSL-300 NMR spectrometer (75.5 MHz; ¹³C). Samples were put into 7 mm ZrO₂ rotors and spun at 4 kHz. Solution NMR spectroscopy was carried out on a Varian Gemini 200 instrument (¹H, 200 MHz; ¹³C, 50.31 MHz). The solvent peak of HOD was set to δ_{H} 4.65.

Scanning electron microscopy was performed with a Philips XL-20 instrument operating at 25 kV with gold-sputtered samples.

Materials

Sodium chloroacetate was purchased from Fluka and recrystallized from ethanol. The other salts were prepared as described either in ref. 3 or as below. The purity of all compounds was checked by elemental analysis (C, H), ¹H and ¹³C NMR spectroscopy in solution, IR spectroscopy (KBr), DSC, X-ray powder diffraction and combined TG-DTA-MS. Special care was taken to assure that no residual halogenoacetic acid was present and that neither polyglycolide nor metal salt had already formed.

Lithium chloroacetate. Preparation from chloroacetic acid and LiOH in ethanol at 25 °C. Anal. Found: C, 23.80; H, 2.20. Calc.: C, 23.92; H, 2.01%. TG-DTA-MS: total mass loss starting at 230 °C of 58.8% (calc. for LiCl: 57.8%), detected mass fragment: *m/z* = 60 (CH₃COOH); ¹H NMR (D₂O), δ 3.85 (CH₂); ¹³C CP MAS solid-state NMR, δ 47.4 (CH₂), 181.4

(COO); IR, ν 3009/2954 (C-H), 1611/1595 (C=O), 1433/1401 (C-H), 1262 (C-O), 946, 935, 788, 688, 576, 516 cm⁻¹.

Lithium bromoacetate. Preparation from bromoacetic acid and LiOH in ethanol at 25 °C. Anal. Found: C, 16.64; H, 1.41. Calc.: C, 16.58; H, 1.39%. TG-DTA-MS: mass loss starting at 250 °C; 40.1% at 330 °C, 45.5% at 400 °C, 54.5% at 700 °C (calc. for LiBr: 40.1%); ¹H NMR (D₂O), δ 3.60 (CH₂); ¹³C CP MAS solid-state NMR, δ 29.0 (CH₂), 181.0 (COO); IR, ν 3013/2958 (C-H), 1586 (C=O), 1425/1394 (C-H, COO), 1223 (C-O), 900, 723, 683, 560 cm⁻¹.

Lithium iodoacetate. Preparation from iodoacetic acid and LiOH in ethanol at 25 °C. Anal. Found: C, 12.29; H, 1.15. Calc.: C, 12.52; H, 1.05%. TG-DTA-MS: mass loss starting at 220 °C; 30% at 270 °C, 70% at 400 °C (calc. for LiI: 30.2%); ¹H NMR (D₂O) δ 3.45 (CH₂); ¹³C CP MAS solid-state NMR, δ 14.2 (CH₂), 181.4 (COO); IR, ν = 3001/2947 (C-H), 1586/1575 (C=O), 1425/1378 (C-H, COO), 1178 (C-O), 851, 679, 542 cm⁻¹.

Potassium bromoacetate. Preparation from bromoacetic acid and KOH in ethanol at 0 °C. Anal. Found: C, 13.36; H, 1.29. Calc.: C, 13.57; H, 1.15%. TG-DTA-MS: total mass loss starting at 250 °C of 32.1% (calc. for KBr: 32.8%), detected mass fragments: *m/z* 59 (CH₃COO), 81 (Br); ¹H NMR (D₂O), δ 3.99 (CH₂); ¹³C NMR (D₂O), δ 31.99 (CH₂), 175.17 (COO); IR, ν 2962 (C-H), 1610 (C=O), 1409/1398 (C-H, COO), 1208 (C-O), 916, 899, 671, 557 cm⁻¹.

Potassium bromoacetate-bromoacetic acid (2/1). Preparation from bromoacetic acid and KOH in 3/2 ratio in ethanol at 25 °C. Anal. Found: C, 14.46; H, 1.50. Calc.: C, 14.60; H, 1.42%. DSC: 123.0 °C, +8.0 kJ mol⁻¹ (melting and decomposition); 129.6 °C, -5.6 kJ mol⁻¹ (recrystallization); 148 °C, -9.3 kJ mol⁻¹ (polymerization); TG-DTA-MS: mass loss of 29% between 130 and 250 °C (calc. for release of 0.5 bromoacetic acid: 28.8%), total mass loss to 350 °C 57.6% (calc. for KBr: 51.7%), detected mass fragment: *m/z* = 58 (CH₂COO); ¹H NMR (D₂O), δ 3.83 (CH₂); ¹³C NMR (D₂O), δ 29.61 (CH₂), 173.69 (COO); IR, ν 3032/3023/2960/2944 (C-H), 1645 (C=O), 1388/1378 (C-H, COO), 1224/1208/1154 (C-O), 916, 895, 707, 667, 555 cm⁻¹.

Rubidium chloroacetate. Preparation from chloroacetic acid and aqueous RbOH (50 mass%) in ethanol at -50 °C. Anal. Found: C, 13.22; H, 1.23. Calc.: C, 13.42; H, 1.13%. TG-DTA-MS: total mass loss starting at 250 °C of 29.3% (calc. for RbCl: 32.4%), detected mass fragment: *m/z* = 59 (CH₃COO); ¹H NMR (D₂O), δ 3.91 (CH₂); ¹³C NMR (D₂O), δ 44.36 (CH₂), 175.29 (COO); IR, ν 2989/2957 (C-H), 1607 (C=O), 1399/1331/1295 (C-H, COO), 1244/1067 (C-O), 935, 916, 767, 672, 570 cm⁻¹.

Rubidium bromoacetate. Preparation from bromoacetic acid and aqueous RbOH (50 mass%) in ethanol at -50 °C. Anal. Found: C, 10.04; H, 0.91; Calc.: C, 10.75; H, 0.90%. DSC: 99 °C, -4.7 kJ mol⁻¹, 142 °C, -21.7 kJ mol⁻¹. TG-DTA-MS: total mass loss starting at 250 °C of 22.6% (calc. for RbBr: 26.0%), visible carbon deposition on the sample after cooling; ¹H NMR (D₂O), δ 3.70 (CH₂); ¹³C NMR (D₂O), δ 32.13 (CH₂), 175.14 (COO); IR, ν 2960 (C-H), 1610 (C=O), 1459/1409/1396/1377/1288 (C-H, COO), 1207/1073 (C-O), 914, 899, 833, 670, 556 cm⁻¹.

Rubidium iodoacetate. Preparation from iodoacetic acid and aqueous RbOH (50 mass%) in ethanol at -50 °C. Anal. Found: C, 8.63; H, 0.74. Calc.: C, 8.87; H, 0.80%. TG-DTA-MS: total mass loss starting at 230 °C of 20.6% (calc. for RbI: 21.4%); ¹H NMR (D₂O) δ 3.46 (CH₂); IR, ν

2954 (C–H), 1597 (C=O), 1412/1376/1316 (C–H, COO), 1162 (C–O), 909, 853, 660, 538 cm^{-1} .

Caesium bromoacetate. This was contaminated with CsBr and polyglycolide, *i.e.* partly reacted. Preparation from bromoacetic acid and CsOH·H₂O in ethanol at -50°C . DSC: 35.4, -26.9 , 81.9°C , $+16.7\text{ kJ mol}^{-1}$ (melting of diglycolide?); IR, ν 2961 (C–H), 1605 (C=O), 1409/1399 (C–H, COO), 1287/1247/1207 (C–O), 916, 849, 672 cm^{-1} .

Caesium iodoacetate. Preparation from iodoacetic acid and CsOH·H₂O in ethanol at -50°C . Anal. Found: C, 7.52; H, 0.70. Calc.: C, 7.56; H, 0.63%. TG–DTA–MS: total mass loss starting at 250°C of 18.0% (calc. for CsI: 18.2%); ¹H NMR (D₂O), δ 3.46 (CH₂); IR, ν 3000/2939 (C–H), 1634/1593 (C=O), 1403/1365 (C–H, COO), 1157 (C–O), 1106, 906, 857, 651 cm^{-1} .

Preparation of polyglycolide. Powdered samples were reacted in a closed glass beaker that was heated with an oil-bath. The reaction temperature was chosen 10–20 K below the onset temperatures from DSC (see Table 2). Reaction times were between 30 and 60 min. The completion of the reaction was conveniently checked by IR spectroscopy (C=O vibrations). The formed metal salts were removed by multiple washing with water, followed by drying in vacuo. Polyglycolide was obtained as a light yellowish powder. It should be kept in a dry box to avoid slow hydrolysis by atmospheric water.

We thank Prof. A. Reller for continuous support. Financial support was granted by the Deutsche Forschungsgemeinschaft and by the Fonds der Chemischen Industrie. We are grateful to Dr. B. Benzler, Mettler-Toledo, for kindly carrying out the thermomechanical experiments and to Prof. H. Lechert for the permission to use the scanning electron microscope.

References

- 1 M. Epple and L. Tröger, *J. Chem. Soc., Dalton Trans.*, 1996, 11.
- 2 M. Epple, H. Kirschnick and J. M. Thomas, *J. Therm. Anal.*, 1996, **47**, 331.
- 3 M. Epple and H. Kirschnick, *Chem. Ber.*, 1996, **129**, 1123.
- 4 M. Epple, U. Sazama, A. Reller, N. Hilbrandt, M. Martin and L. Tröger, *Chem. Commun.*, 1996, 1755.
- 5 M. Epple and H. Kirschnick, *Chem. Ber.*, 1997, **130**, 291.
- 6 M. Epple and H. Kirschnick, *Liebigs Ann. Chem.*, 1997, 81.
- 7 J. Vasenius, P. Helevirta, H. Kuisma, P. Rokkanen and P. Törmälä, *Clinical Mater.*, 1994, **17**, 119.
- 8 G. O. Hofmann, *Arch. Orthopaedic Trauma Surgery*, 1995, **114**, 123.
- 9 C. C. Chu, in *ACS Symp. Ser.*, ed. T. L. Vigo, ACS, Washington, DC, 1991, vol. 457.
- 10 R. Ries and F. Moll, *Eur. J. Pharm. Biopharm.*, 1994, **40**, 14.
- 11 *Handbook of Polymer Synthesis*, ed. H. R. Kricheldorf, Marcel Dekker, New York, 1992.
- 12 L. Elizabé, B. M. Karinki, K. D. M. Harris, M. Tremayne, M. Epple and J. M. Thomas, unpublished work.
- 13 W. E. Brown, D. Dollimore and A. K. Galwey, *Reactions in the Solid State*, Elsevier, Amsterdam, 1980.
- 14 H. Schmalzried, *Chemical Kinetics of Solids*, VCH, Weinheim, 1995.
- 15 R. Ginde and R. Gupta, *J. Appl. Polym. Sci.*, 1987, **33**, 2411.
- 16 J. Pokorny, *Sb. Vys. Sk. Chem.-Technol. Praxe, B: Anorg. Chem. Technol.*, 1972, **14**, 127.
- 17 J. Pokorny, *Sb. Vys. Sk. Chem.-Technol. Praxe, B: Anorg. Chem. Technol.*, 1972, **14**, 153.
- 18 M. Epple, H. Kirschnick, G. N. Greaves, G. Sankar and J. M. Thomas, *J. Chem. Soc., Faraday Trans.*, 1996, **92**, 5035.
- 19 G. W. H. Höhne, H. K. Cammenga, W. Eysel, E. Gmelin and W. Hemminger, *Thermochim. Acta*, 1990, **160**, 1.
- 20 H. K. Cammenga, W. Eysel, E. Gmelin, W. Hemminger, G. W. H. Höhne and S. M. Sarge, *Thermochim. Acta*, 1993, **219**, 333.
- 21 S. M. Sarge, E. Gmelin, G. W. H. Höhne, H. K. Cammenga, W. Hemminger and W. Eysel, *Thermochim. Acta*, 1994, **247**, 129.

Paper 7/00275K; Received 13th January, 1997